Marine Pollution Bulletin xxx (xxxx) xxx–xxx

Contents lists available at ScienceDirect

Marine Pollution Bulletin

journal homepage: www.elsevier.com/locate/marpolbul

Effects of ocean acidification on the shells of four Mediterranean gastropod species near a CO_2 seep

Ashley Duquette[a], James B. McClintock[a,*], Charles D. Amsler[a], Alberto Pérez-Huerta[b], Marco Milazzo[c], Jason M. Hall-Spencer[d]

[a] Department of Biology, University of Alabama at Birmingham, Birmingham, AL 35294, USA
[b] Department of Geological Sciences, University of Alabama, Tuscaloosa, AL 35487, USA
[c] Dipartimento di Scienze della Terra e del Mare, University of Palermo, 90123 Palermo, Italy
[d] Marine Biology and Ecology Research Centre, School of Marine Science and Engineering, Plymouth University, Plymouth, UK

ARTICLE INFO

Keywords:
CO2 seep
Ocean acidification
Gastropods
Shell
Mineral
Mediterranean

ABSTRACT

Marine CO_2 seeps allow the study of the long-term effects of elevated pCO_2 (ocean acidification) on marine invertebrate biomineralization. We investigated the effects of ocean acidification on shell composition and structure in four ecologically important species of Mediterranean gastropods (two limpets, a top-shell snail, and a whelk). Individuals were sampled from three sites near a volcanic CO_2 seep off Vulcano Island, Italy. The three sites represented ambient (8.15 pH), moderate (8.03 pH) and low (7.73 pH) seawater mean pH. Shell mineralogy, microstructure, and mechanical strength were examined in all four species. We found that the calcite/aragonite ratio could vary and increased significantly with reduced pH in shells of one of the two limpet species. Moreover, each of the four gastropods displayed reductions in either inner shell toughness or elasticity at the Low pH site. These results suggest that near-future ocean acidification could alter shell biomineralization and structure in these common gastropods.

1. Introduction

Ocean acidification (OA) is a key environmental factor driven by anthropogenic combustion of fossil fuels (IPCC, 2013; Hoegh-Guldberg et al., 2014) that has both indirect or direct effects on biomineralization processes in calcified marine invertebrates, challenging the capacity to grow, reproduce, calcify, and maintain essential acid-base balances (Kroeker et al., 2013a; Bray et al., 2014; Dubois, 2014; Lardies et al., 2014; Gaylord et al., 2015). Marine invertebrate taxa exhibit varying responses to increased seawater acidification and reductions in the saturation state of the polymorphs of calcium carbonate, aragonite and calcite. Given their important ecological roles and their value as environmental biomonitors, mollusks have been of interest in regards to ocean acidification. Some mollusks have demonstrated positive (increased calcification, increased rate of calcification and/or growth) or parabolic (positive net calcification under intermediate acidification but negative under high acidification) reactions to increased acidity (Ries et al., 2009; Rodolfo-Metalpa et al., 2011). In contrast, the majority of studies to date have detected negative impacts of acidification on mollusk biomineralization. Such responses include net shell dissolution (bivalves: Green et al., 2004; gastropods: Hall-Spencer et al., 2008), reduced shell growth or decreased calcification rates (gastropods: Shirayama and Thornton, 2005; Melatunan et al., 2013; bivalves: Gazeau et al., 2007; Ries et al., 2009), and impaired shell integrity (Green et al., 2004; Beniash et al., 2010; Fitzer et al., 2014). These effects are typically greater in species lacking a thick organic layer (periostracum) covering their shells (e.g., Rodolfo-Metalpa et al., 2011; Coleman et al., 2014).

Most ocean acidification research to date has been short-term and laboratory-based. These studies suggest that OA impacts are likely to be species-specific with a few species benefitting, but many others being negatively impacted either through direct or indirect effects of rising CO_2 levels (Gaylord et al., 2015). Despite the value of such research, it is difficult to extrapolate the observed effects of ocean acidification on calcifying marine invertebrates that occur in coastal ecosystems. Accordingly, the use of shallow submarine CO_2 seeps provide opportunities for the study of the long-term biotic effects of increasing pCO_2 levels (Hall-Spencer et al., 2008). Studies at CO_2 seeps in the Mediterranean, Japan, and Papua New Guinea have revealed significant reductions in the biodiversity of marine invertebrates under acidified conditions, as well as shifts in trophic structure and simplified food webs (Cigliano et al., 2010; Inoue et al., 2013; Kroeker et al., 2013b;

* Corresponding author.
E-mail address: mcclinto@uab.edu (J.B. McClintock).

http://dx.doi.org/10.1016/j.marpolbul.2017.08.007
Received 7 September 2016; Received in revised form 2 August 2017; Accepted 4 August 2017

Fabricius et al., 2014; Baggini et al., 2015). Much of this decline in biodiversity is due to reductions in the presence of calcifying marine organisms including scleractinian corals, mollusks and echinoderms (Inoue et al., 2013; Fabricius et al., 2014; Garilli et al., 2015). Species that do survive under acidified conditions may become more vulnerable to predation due to weakened shells/skeletons and are often smaller due to dissolution or physiological stress (Rodolfo-Metalpa et al., 2015; Langer et al., 2014; Collard et al., 2016; Newcomb et al., 2015; Harvey et al., 2016).

The overall aim of the present study was to determine whether chronic exposure to elevated CO_2 alters the mineralogy, structure, and strength of the shells of four common species of sympatric gastropods (two limpets, a top-shell snail, and a whelk) at three sites near a natural CO_2 seep. An understanding of the comparative vulnerability of these four common gastropods will facilitate predictions about their future respective trophic and ecological roles in the community. The two limpets *Patella rustica* Linnaeus, 1758 and *P. caerulea* Linnaeus, 1758 have a pattern of distinct zonation with the former found exclusively in the upper intertidal, and the latter inhabiting the lower mid-littoral (Della Santina et al., 1993). This not only separates them in terms of their degree of exposure to OA, but also their respective vulnerability to predators. The other two gastropods, the carnivorous whelk *Hexaplex trunculus* Linnaeus, 1758 and the top shell *Osilinus turbinatus* Van Born, 1778, both occur in the mid-littoral zone (Morton et al., 2007; Boucetta et al., 2010). All four gastropod species have a trochophore and veliger larva and thus recruit to the benthos via a planktonic larva.

To conduct a comparative evaluation of the properties of shells of these four species of gastropods at various distances from a natural CO_2 seep we assessed shell mineralogy (percent calcite and percent aragonite) based on X-ray diffraction (XRD) analysis. Furthermore, using scanning electron microscopy (SEM) and electron backscatter diffraction (EBSD) we determined shell microstructure. Finally, we evaluated shell mechanical strength based on point compression to determine the force to fracture the shell, along with shell toughness, and elasticity.

2. Methods

2.1. Collection sites

Our study site was a CO_2 seep system located in the shallow, nearshore waters of Vulcano Island approximately 25 km north of Sicily, Italy (Boatta et al., 2013). Gastropods were collected from three field stations (designated from this point forward as Ambient, Moderate, and Low pH sites) off the northeastern coast of Levante Bay, northeastern Vulcano Island (Fig. 1). Levante Bay is a shallow (2–3 m depth), micro-tidal region that contains active CO_2 seeps which create a pH gradient (~6.8–8.2 pH_{NBS} units) along the northeastern shoreline (Boatta et al., 2013). The seawater pH_{NBS} and carbonate chemistry at the three stations was defined by Milazzo et al. (2014), and based on data collected during 2011–2012. The Ambient site served as a reference site with a mean pH of 8.15 ± 0.01 (n = 95) and was located approximately 850 m from the main CO_2 seep; the Moderate site was approximately 390 m distant from the seep with a mean pH of 8.03 ± 0.01 (n = 95) which is a predicted near-future level of pH (Nakicenovic and Swart, 2000); the Low site was approximately 300 m distant from the seep with a mean pH of 7.73 ± 0.02 (n = 95), predicted to occur by the end-of-century (IPCC, 2013; Milazzo et al., 2014).

It is important to note that these three study sites do not vary significantly from one another in terms of seawater temperature, light, total alkalinity, and salinity (Boatta et al., 2013; Milazzo et al., 2014). As heavy metal pollution can be a confounding issue in close proximity to CO_2 seeps (Roberts et al., 2013), it is also important that in an evaluation of heavy metal pollution across a distance from the seep, Vizzini et al. (2013) determined that all sites located further than about

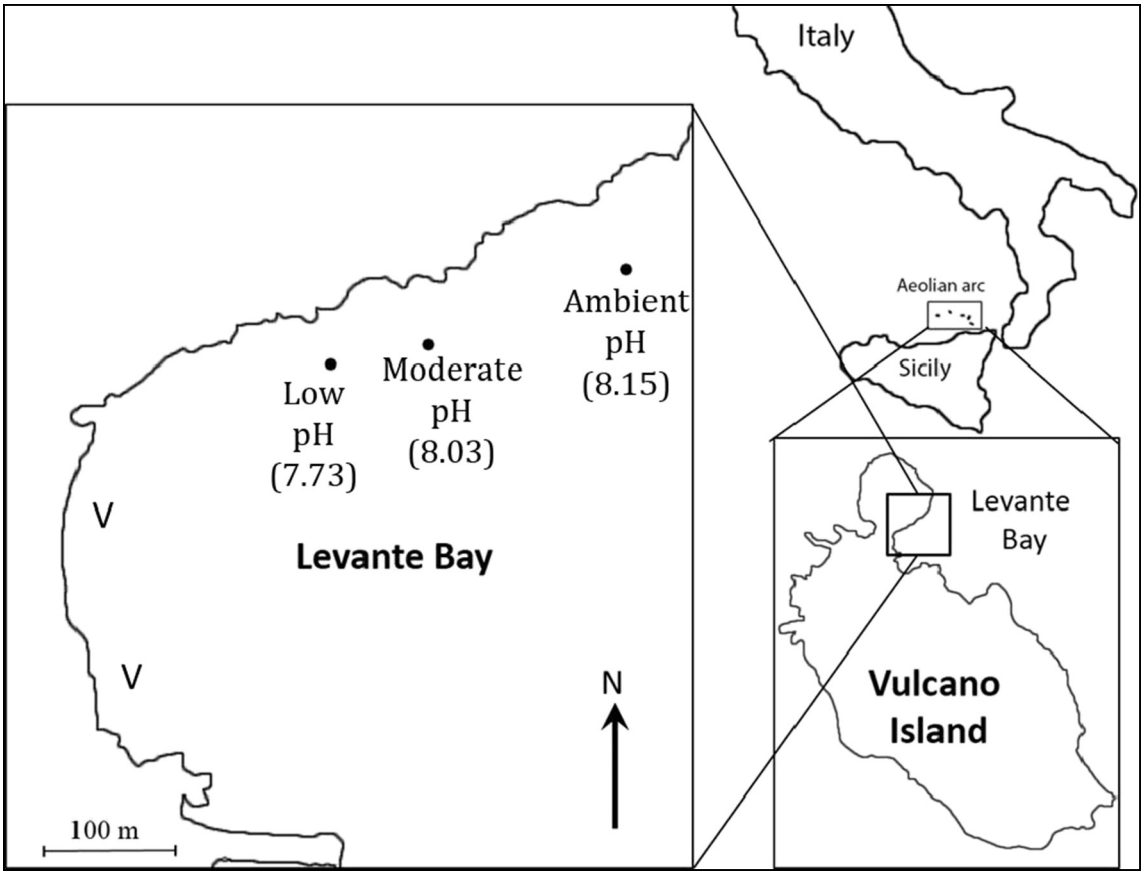

Fig. 1. Location of sampling sites along the northeastern shore of Levante Bay, Vulcano Island, Italy. The "V" represents locations of CO_2 seeps.

Table 1
Total sample sizes of shells and their mean length (± SE) for each of four gastropod species collected at ambient, moderate, and low pH seep sites. Also shown are the sample sizes and mean length (± SE) of shells examined from each pH site for X-ray diffraction (XRD) and strength analyses.

Species	pH	Total sample size (N)		XRD analysis		Strength analysis	
			Mean (± 1 SE) shell size (mm)	Sample size (N)	Mean (± 1 SE) Shell Size (mm)	Strength sample size (N)	Mean (± 1 SE) shell size (mm)
Whelk *H. trunculus*	Ambient	24	43.5 ± 1.2	13	42.9 ± 1.4	9	45.8 ± 2.3
	Moderate	34	42.5 ± 1.9	13	38.7 ± 2.1	0	0
	Low	25	40.0 ± 1.1	14	40.0 ± 1.6	9	40.4 ± 1.7
Top-shell *O. turbinatus*	Ambient	50	10.8 ± 0.4	15	11.5 ± 0.8	12	11.1 ± 0.5
	Moderate	31	12.1 ± 1.2	15	12.7 ± 1.7	0	0
	Low	28	8.7 ± 0.4	16	9.3 ± 0.5	9	8.6 ± 0.7
Limpet *P. caerulea*	Ambient	20	19.2 ± 0.7	11	18.4 ± 0.9	7	20.1 ± 1.0
	Moderate	31	21.0 ± 0.6	21	21.6 ± 0.7	0	0
	Low	47	21.9 ± 0.8	25	20.8 ± 0.8	17	24.5 ± 1.7
Limpet *P. rustica*	Ambient	81	15.9 ± 0.4	23	16.9 ± 0.8	23	18.0 ± 0.4
	Moderate	32	16.2 ± 0.6	22	17.1 ± 0.6	0	0
	Low	35	18.5 ± 0.9	16	18.5 ± 0.9	15	19.9 ± 1.3

300 m from the CO_2 seep were in generally 'good' (levels unlikely to be harmful) condition in terms of the heavy metal pollution (Ba, Fe and trace elements As, Cd, Co, Cr, Cu, Hg, Mn, Mo, Ni, Pb, V, and Zn). None of the three sites examined in the present study were located < 300 m of the seep (see distances above).

Every gastropod encountered (all sizes) was collected haphazardly by hand while snorkeling in May 2013 at the three sites described above. Collections focused on removing all gastropods within an area of approximately 15 m × 15 m at each site. Site-specific sample sizes of gastropods at the time of collection were: *P. caerulea* (Ambient: $n = 20$; Moderate: $n = 31$; Low: $n = 47$), *P. rustica* (Ambient: $n = 81$; Moderate: $n = 32$; Low: $n = 35$), *O. turbinatus* (Ambient: $n = 50$; Moderate: $n = 31$; Low: $n = 28$), *H. trunculus* (Ambient: $n = 24$; Moderate: $n = 34$; Low: $n = 25$). All collected individuals of each species were placed into zip-lock bags, sealed, then placed inside tightly capped 2-liter plastic bottles, and transported to the University of Alabama at Birmingham, USA. Immediately upon arrival, the gastropods were removed from their shells and their respective soft tissues placed into labeled, 250 mL plastic jars with a solution of 4% formalin. All shells were rinsed repeatedly under flowing, distilled water and gently scrubbed clean by hand, labeled, and then air dried and digitally photographed using a Nikon D5100 digital camera. For each shell, length, width, height, and shell aperture width and height were measured to the nearest tenth of a millimeter using a digital caliper (iGaging 6″ External Caliper). All shell length data were used for intraspecific comparisons of the mean sizes of individuals of each gastropod species at each of the three seep sites.

The numbers of shells examined varied with the type of analysis. A quantitative approach was taken for determinations of shell mineralogy and shell strength (point compression). Numbers of shells examined for mineralogy using X-ray diffraction ranged from 11 to 25 for a given site, while sample sizes of shells used for shell strength analysis (Ambient and Low sites only) ranged from 7 to 23 for a given site (Table 1). Shells for these analyses were randomly selected from the pool of available shells by numbering all of them and using a random number generator in Microsoft Excel to choose those for analysis. A qualitative approach was taken for scanning electron microscopy and electron backscatter diffraction carried out on a representative shell from each of the three sites. Individuals on the extreme ends of shell condition were removed from consideration and a randomly selected individual was chosen from the remaining shells to be a representative shell for these two analyses (one shell per species per site).

2.2. X-ray diffraction analysis (XRD)

Shells of each gastropod species were examined for their mineralogy (aragonite and calcite in both limpets; only aragonite in the top-shell snail and whelk) by X-ray diffraction (Ries, 2011). Shells were prepared by repeatedly submerging each shell in a 10% NaClO solution to digest away all residual organic tissue (McClintock et al., 2011). Clean shells were rinsed under distilled water, and then air-dried for a period of 12 h. Shells were wrapped in sterile gauze and broken into fragments with a hammer. Fragments were subsequently placed into an agate mortar along with one to two mL of 95% ethanol and then ground to a slurry with an agate pestle. The resultant slurry was placed onto a 25 mm × 75 mm × 1 mm glass microscope slide and air dried for 12 h to a powder.

Powdered shell was analyzed using a Philips X'Pert Analytical X-ray diffraction system (PANalytical B.V., Almelo, Netherlands). X-ray diffraction data were collected at 45 kV and 40 mA, and the 2Θ scan range was from 25° to 50°, with a step size of 0.06 and scan speed of 2 s $step^{-1}$ to obtain precise measurements of calcite and aragonite peaks. The resulting X-ray diffraction pattern for each shell was used to determine the levels (percent) of calcite and/or aragonite using equations given in Ries (2011). The primary calcite peak (d(104)) corresponded to 2Θ = 29.5–30.2° on the X-ray diffraction pattern generated. The two primary aragonite peaks (d(111) and d(021)) corresponded to 2Θ = 26.3° and 27.2°, respectively (Milliman, 1974).

2.3. Scanning electron microscopy (SEM) and electron backscatter diffraction (EBSD) analyses

Whole shells of representative individuals from each gastropod species from the Ambient and Low sites were examined using scanning electron microscopy and electron backscatter diffraction by first immersing each shell in epoxy resin (EpoThin Epoxy System) followed by a curing period of at least 24 h at room temperature. Epoxy-embedded shells were then cut in half longitudinally using a diamond tipped saw. The exposed surface of the embedded shell was then ground and polished for analysis following the protocol described in Pérez-Huerta and Cusack (2009) excluding the use of colloidal silica. One-half of a shell from each species from the Ambient and Low sampling sites was examined using scanning electron microscopy. The other half of the same shell from each individual was examined using electron backscatter diffraction, which is a technique that is complementary to SEM and provides a higher resolution capacity to evaluate crystal orientation and texture.

Resin-embedded shell halves for scanning electron microscopy analysis were etched with 2% HCl for a period of 30 s, generously coated with gold using a sputter coater so as to account for shell curvature, and imaged using a Quanta FEG 650 Scanning Electron Microscope (FEI) (working distance = 10 mm) set on high-vacuum

mode at 20 kV with a spot of four. Our use of an elevated 20 kV was based on the assumption that the structures (cross sections) had some depth and facilitated the acquisition of valid information. Scanning electron microscopy images were collected from the apex region of the limpet shell halves. The apex of the shell is the oldest portion of the shell and erosion becomes evident at this location first. Images for the shell halves of top-shell snails and whelks were collected for a single uniform ventral location on the first shell whorl above the aperture.

Shell halves for electron backscatter diffraction analysis were coated with a 2.5 nm layer of carbon and the epoxy resin surrounding each shell hand-painted with silver paint to decrease electron charging (see Pérez-Huerta and Cusack, 2009). Electron backscatter diffraction was carried out with a Hikari EDAX camera mounted on a Field Emission Scanning Electron Microscope (Tescan Lyra XMU). OIM 7.0 software was employed to collect data at 30 kV, under a high vacuum mode, large beam intensity (20), and at a step size resolution of 1 μm or less. Electron backscatter diffraction images were collected from the apex of the representative limpet shells. Electron backscatter diffraction data were analyzed using OIM 5.3 from EDAX-TSL and presented in diffraction maps and crystallographic maps, with different colors representing different crystal orientations within a given region of shell (further details in Pérez-Huerta et al., 2011).

2.4. Shell strength analysis

Replicate shells of individuals of each gastropod species collected from the Ambient and Low sample sites were used for mechanical strength analysis. Shells were cut with a diamond saw such that portions of both the external and internal surfaces of the shell were isolated for analysis. Shells of the two species of limpets were cut horizontally, at two-thirds of the shell's length as measured from the anterior tip. The apex of limpet shells was selected as the site for measures of external shell surface strength. The internal shell surface was tested at a site approximately 1–3 mm (adjusted proportionately to the total length of the shell) from the posterior tip of the shell.

Shells of the top-shell snail and the whelk were cut horizontally above the aperture to expose the inner shell surface. Point compression was tested for the inner surface of each shell at a standardized location halfway across the length, and 4 mm from the lip, of the aperture. The shell apex was selected for measurements of external shell strength for the top-shell snail. For the whelk, the surface of the shell's whorl, directly above the aperture, was used for measures of the external shell strength. Prior to shell strength measurements, each shell sample was embedded in resin such that only the outer and inner shell surfaces described above were left exposed. The limpet shells were embedded in JB Weld epoxy. The shells of the top-shell snail and the whelk were embedded in EpoThin Epoxy Resin rather than JB Weld because the latter was too viscous to fill the whorls of the shells.

Shell mechanical strength analyses were conducted using a point compression measure of the force necessary to crack a given shell. This technique also allowed for indirect calculations of shell toughness and shell elasticity. For each point compression analysis, a shell sample was placed onto the flat stage of a force stand (LRX *Plus*, Lloyd Instruments) and the compression measure performed using a metal point affixed to the stand. A 5-kN load cell was used with the metal point lowered at a speed of 0.03 mm·min^{-1} for shells of both limpets and at a speed of 0.06 mm·min^{-1} for shells of the top-shell snail and whelk. During each run, the point was lowered until shell fracture occurred. The force exerted on the shell during the run and the machine extension (distance the machine arm moved between readings) was continuously recorded using NEXYGENPlus software. Data derived from force and machine extension measures were used to determine Young's Modulus (elasticity) via stress-strain curves employing the following equations:

$$\text{Stress} = \sigma = \frac{F}{A}$$

$$\text{Strain} = \varepsilon = \frac{\Delta L}{L_e}$$

where F is force (N) at a given time point; A is the area (m^2) of the metal point used for the compression test; ΔL is the machine extension (m), and L_e is the effective length (m). Elasticity was calculated as the slope between two points of the linear portions of the stress-strain curves ($\Delta\sigma/\Delta\varepsilon$) for each shell analyzed. The amount of energy per unit volume the shell withstands before breaking (toughness; J·m^{-3}) was calculated as the area under the stress-strain curve.

2.5. Statistical analyses

Mean shell lengths of all individuals collected from the Ambient, Moderate, and Low sites were compared within each of the four gastropod species. Shell length data that were normally distributed were compared using an ANOVA followed by a *post-hoc* Tukey test. For shell length data that was not normally distributed, log transformed data were subjected to a nonparametric Kruskal-Wallace rank sum test followed by a Dunn's test.

For data generated from XRD analysis, covariance of mean percent (± 1 SE) of calcite and aragonite with both site (Ambient, Moderate, and Low) and size (shell length) was tested using a linear regression model. The mean percent (± 1 SE) of calcite and aragonite were compared across the three sites (pH) for both of the limpet species. These data were not normally distributed and were therefore subjected to a Kruskal-Wallis test followed by a Dunn's test. As the top-shell snail and the whelk were composed entirely of aragonite, no site comparisons were necessary.

Shell mechanical strength data were compared separately for internal and external shell surfaces for each of the four gastropod species. For each shell surface type, data were compared between the Low and the Ambient sites for three shell structure measures (force, toughness, and elasticity). Covariance of these variables with both site (pH) and size (shell length) was determined using a linear regression model. There were several cases in which the data were adjusted for shell size (length) because a covariance between site (pH) and size (shell length) was detected. These included both the toughness and elasticity of the external shell surface in the limpet *P. rustica,* the force required to break the internal shell surface in the top-shell snail *O. turbinatus*, and the toughness of and force required to break the internal shell surface in the whelk *H. trunculus*. Normally distributed data were compared between the Ambient and Low sites using a Student's *t*-test. Data that were not normally distributed were compared using a Mann-Whitney *U* test. R 3.3.1 Statistical Software (R Development Core Team, 2016) was used to conduct all statistical analyses and a $p < 0.05$ was considered significant.

3. Results

Mean ± 1 SE sizes (shell length) of the four species of gastropod intensively collected (every individual encountered was collected) from each of the three pH sites are presented in Fig. 2. Mean shell length did not differ significantly among the three pH sites in the limpet, *P. caerulea,* (ANOVA, $F_{(2,95)} = 2.717$, $p = 0.071$) and the whelk *H. trunculus* (Kruskal-Wallis test, $H_2 = 2.95$, $p = 0.229$). However, mean shell length differed significantly between sites for the limpet, *P. rustica,* (ANOVA, $F_{(2126)} = 4.05$, $p = 0.02$) and the top-shell snail *O. turbinatus* (Kruskal-Wallis test, $H_2 = 9.07$, $p = 0.011$). Specifically, shells of the limpet *P. rustica* were, on average, longer at the Low site than those at the Ambient site (Tukey HSD test, $p = 0.015$). In contrast, shells of top-shell snail collected from the Low site were, on average, shorter than those at the Ambient site (Dunn's test, $p = 0.0013$).

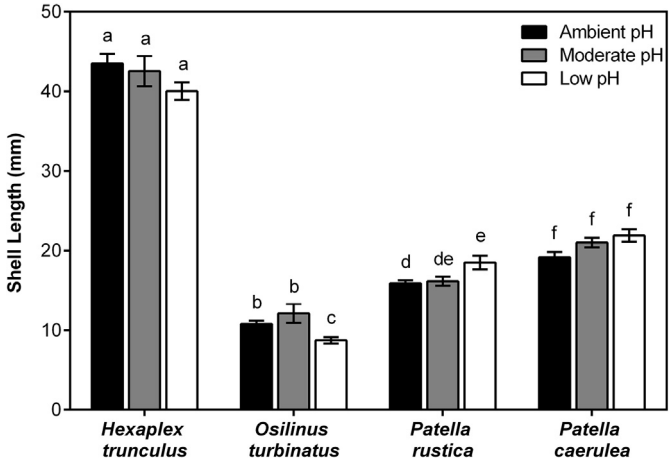

Fig. 2. Mean shell length for four species of gastropods collected from ambient, moderate, and low pH sites in shallow water off Vulcano. Error bars ± SE mm. Lowercase letters represent significant differences in mean shell lengths for each species for each of the three seep sites.

3.1. X-ray diffraction

X-ray diffraction analysis for three of the gastropod species agreed with previous studies reporting that the shells of the limpets, *P. caerulea* and *P. rustica* were both composed of aragonite and calcite (Lécuyer et al., 2012; Langer et al., 2014. We found the shell of the topshell *Osilinus turbinatus* was composed entirely of aragonite as reported by Mannino et al. (2008). We report herein the first analysis of the mineralogy of the whelk *Hexaplex trunculus* whose shell we found to also be entirely constructed of aragonite.

For the two limpets whose shells contained both polymorphs of calcium carbonate we found mean (± 1 SE) percent calcite and aragonite ranged from 96.2 ± 0.97 to 97.7 ± 0.69 and 2.3 ± 0.69 to 3.8 ± 0.97, respectively, for *P. caerulea*. Mean ± 1 SE percentages of aragonite and calcite in shells did not differ significantly with site for *P. caerulea* (Kruskal-Wallis test, $H_2 = 1.143$, $p = 0.5647$), but differed significantly by site for *P. rustica* (Kruskal-Wallis test, $H_2 = 13.569$, $p = 0.0011$) (Fig. 3). Mean (± 1 SE) percent calcite and aragonite ranged from 84.5 ± 1.6 to 94.6 ± 1.3 and 5.4 ± 1.3 to 15.6 ± 1.6, respectively, for *P. rustica*. Significant differences in the ratios of calcite to aragonite were found in the shells of *P. rustica* collected at the Low site as compared to the Moderate site (Dunn's test, $p = 0.0004$). Levels of aragonite in shells of limpets from the Low site were about a third (5.4% versus 15.6%) of those in shells of individuals from the Moderate site (Fig. 3).

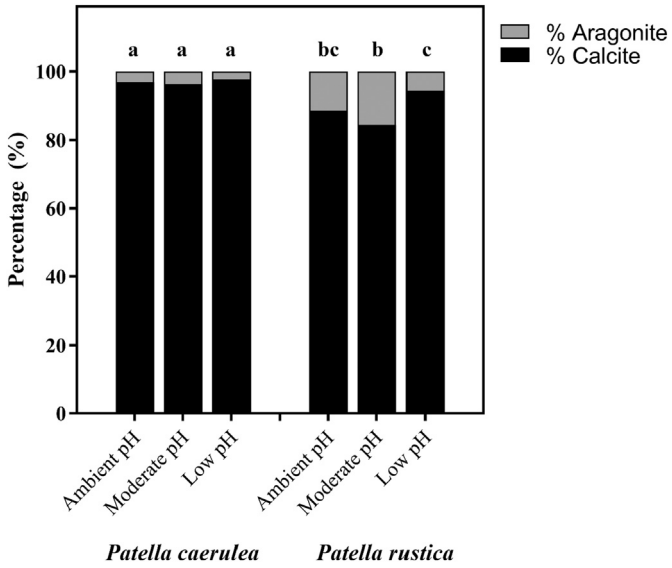

Fig. 3. Percentages of aragonite and calcite in the shells of the limpets *Patella rustica* and *P. caerulea* collected from ambient, moderate, and low pH sites off Vulcano. Lowercase letters indicate significant differences in the ratio of aragonite to calcite in shells within a given species. Comparisons were made only within, not between, species.

3.2. Shell Imaging

Digital photographs of shells collected from each of the three pH sites revealed varying levels of dissolution among the four species of gastropods. Randomly selected individuals were chosen as representatives of each species from all three study sites (Fig. 4). Shells of the whelk *H. trunculus* collected at the Low site showed the most dramatic shell dissolution with considerable pitting and erosion of the outermost layer (Fig. 4a–c). In some instances, whelk shells from this site displayed irregularly shaped holes that measured up to 5 mm diameter. The top-shell snail and the sublittoral limpet *P. caerulea* showed a similar, but more modest level of shell dissolution that increased with proximity to the Low site. Shells of both species from the Moderate site had reduced luster and faded pigmentation, while shells at the Low site displayed mild dissolution of the outermost layer (Fig. 4: d–f; j–l respectively). Slight shell dissolution was evident at the shell apex (oldest region) of the intertidal limpet *P. rustica* at the Low site, but was less evident at the other two sites (Fig. 4g–i).

Scanning electron microscopy indicated qualitatively that each representative shell from each site of the bimineralic limpets' *P. caerulea* and *P. rustica* had an outer prismatic calcite layer above an inner crossed-lamellar aragonite layer (Fig. 5a–b). The representative shells of the entirely aragonite top-shell snail and whelk were found to be constructed of multiple layers. While the whelk had only crossed-lamellar microstructure evident, the top-shell snail had both prismatic and crossed-lamellar microstructures present (Fig. 5c–d).

Electron backscatter diffraction images of a representative shell of the limpet *P. caerulea* collected from the Low site revealed qualitatively an increased disorganization of the crystallography of the calcite layer (Fig. 6). The outermost edge of the representative shell collected from the Ambient site displays a thin layer (< 20 μm) of small, irregularly shaped calcite crystals (Fig. 6a–b). These crystals show a preferred (most common) crystallographic orientation with the *c*-axis parallel to the outermost edge of the shell. This outermost shell layer of the individual from the Ambient site was separated from an inner calcite layer by a distinct organic layer (Fig. 6a). The inner sublayer of the calcite layer was composed of larger, prismatic crystals oriented with the *c*-axis perpendicular to the outermost shell layer (Fig. 6b). A transition from the outer calcite layer to the inner aragonite layer is denoted by progression to a region of discontinuous diffraction. The representative shell of an individual from the Low site had a single thinner, more disorganized calcite layer (Fig. 6d–e), without the prismatic layer and the outermost thinner layer. The preferred crystallographic orientation is with the *c*-axis parallel to the horizontal plane of the shell.

Electron backscatter diffraction images of representative shells of the limpet *P. rustica* collected from the Ambient and Low sites revealed relatively similar shell crystallography at both sites (Fig. 7). While the shell from the Ambient site had overall lower electron diffraction (Fig. 7a), it is evident that two discrete portions make up the calcite layer: an outer sublayer with smaller crystals oriented with the *c*-axis parallel to the outermost edge of the shell, and an inner sublayer composed of larger crystals with a preferred orientation with the *c*-axis perpendicular to the outermost edge of the shell (Fig. 7b). The same two sublayers within the calcite layer are even more obvious within the shell of a representative individual collected from the Low site (Fig. 7d–e). The outer sublayer of the calcite layer is composed of small, irregularly shaped crystals, which demonstrate a preferred orientation with the *c*-axis parallel to the outermost edge of the shell. The inner

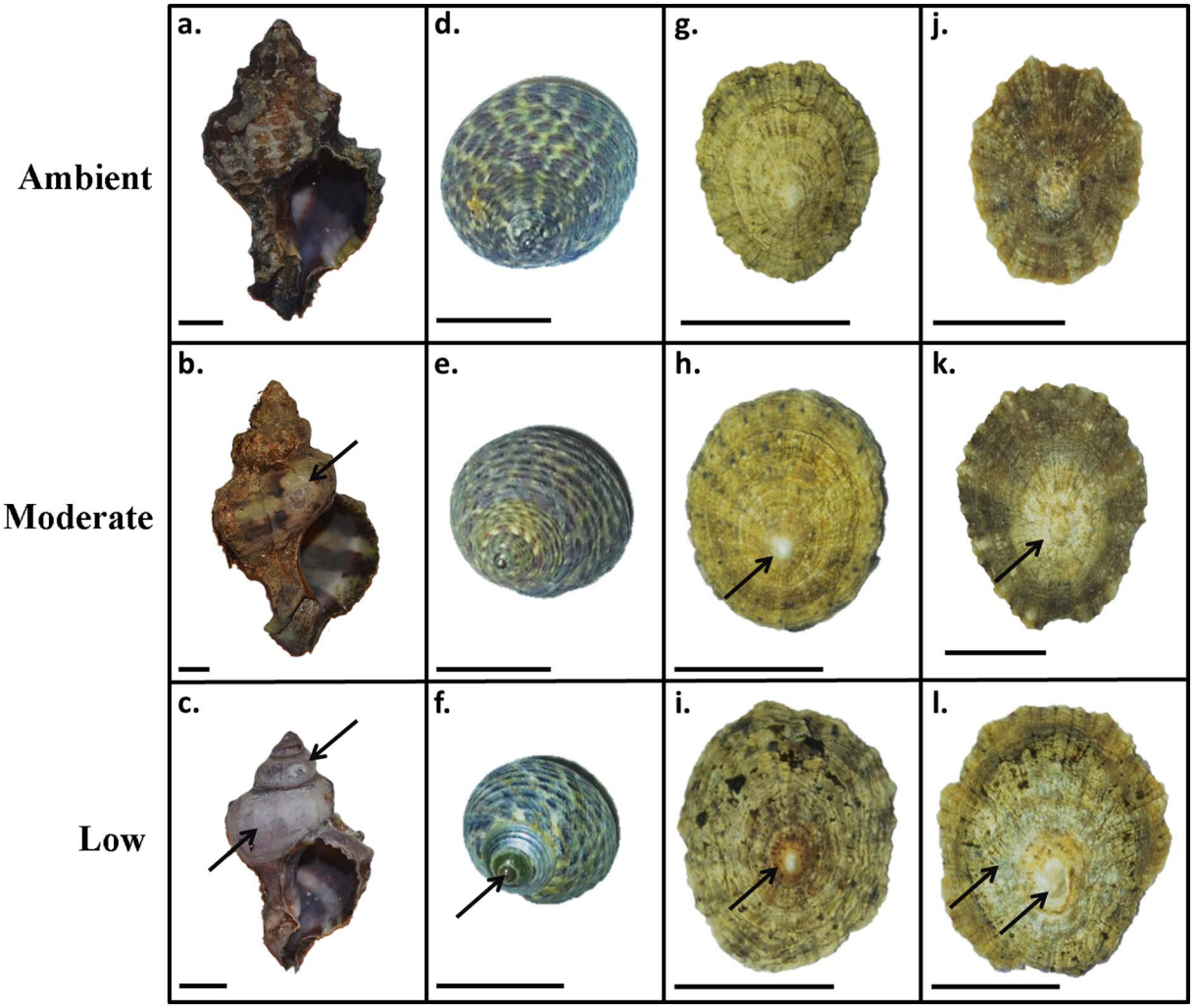

Fig. 4. Representative digital photographs of shells collected from ambient (row 1), moderate (row 2), and low (row 3) pH sites off Vulcano for the gastropods *Hexaplex trunculus* (a–c), *Osilinus turbinatus* (d–f), *Patella rustica* (g–i), and *Patella caerulea* (j–l). Scale bars for each picture represent 1 cm. Arrows indicate areas of visible dissolution.

sublayer of the calcite layer is less well defined, but is composed of larger crystals oriented with the *c*-axis perpendicular to the outermost edge of the shell. There is no obvious simplification of the crystallographic structure of the calcite layer within the shell of *P. rustica* at the Low site (Fig. 7d). There does appear, however, to be some loss of organization of the inner (and newer) portion of the calcite layer in the shell from the representative individuals from the Low site (Fig. 7e).

3.3. Shell strength characteristics

The mean force required to fracture the shell did not differ significantly between the Ambient and Low sites for any of the four gastropod species for either the external (*P. caerulea:* $p = 0.5242$; *P. rustica:* $p = 0.6349$; *O. turbinatus:* $p = 0.8506$; *H. trunculus:* $p = 0.2905$; Fig. 8a) or internal surfaces (*P. caerulea*: $p = 0.355$; *P. rustica*: $p = 0.650$; *O. turbinatus*: $p = 0.118$; *H. trunculus*: $p = 0.574$; Fig. 8b). The mean shell toughness ($J{\cdot}m^{-3}$) of external shell surfaces also did not differ significantly between shells of individuals from the Ambient and Low sites for any of the gastropod species (*P. caerulea:* $p = 0.6207$; *P. rustica:* $p = 0.9362$; *O. turbinatus:* $p = 0.8586$; *H. trunculus:* $p = 0.8672$; Fig. 8c). In contrast, the mean shell toughness of internal shell surfaces differed significantly between the two sites for two of the four gastropod species, the limpet *P. rustica* (*t*-test, $t_{35} = 2.776$, $p = 0.009$) and the whelk *H. trunculus* (*t*-test, $t_{14} = 2.565$, $p = 0.022$) (Fig. 8d). Inner surfaces of shells of the limpet *P. rustica* collected from the Low site had significantly higher toughness values than those of individuals collected at the Ambient site. In contrast, inner surfaces of the whelk shells collected from the Low site had significantly lower toughness values than those of individuals collected at the Ambient site.

A significant difference in the mean elasticity (ability to deform and rebound) of the external shell surface was detected in the top-shell snail (*t*-test, $t_{18} = 2.423$, $p = 0.026$), but not among any of the three other species (*P. caerulea:* $p = 0.639$; *P. rustica:* $p = 0.629$; *H. trunculus:* $p = 0.431$; Fig. 8e). The external surface elasticity was significantly reduced in top-shell snail shells from individuals at the Low site (0.25 ± 0.02 GPa; $n = 8$) when compared to those from the Ambient site (0.34 ± 0.02 GPa; $n = 12$). Both species of limpets had inner shell surfaces with significantly lower elasticity at the Low site (*P. caerulea*: *t*-test, $t_{21} = 2.736$, $p = 0.012$; *P. rustica*: *t*-test, $t_{35} = 4.45$, $p < 0.0001$; Fig. 8f). Mean elasticity of the inner shell surface did not differ significantly among shells of individuals of the top-shell snail (*t*-test, $t_{15} = 0.639$, $p = 0.533$) or whelk (*t*-test, $t_{14} = 1.127$, $p = 0.279$) collected from the Ambient and Low sites (Fig. 8f).

4. Discussion

The present study is consistent with the consensus that there is a wide degree of species-specific variation in responses of marine mollusks to ocean acidification (Parker et al., 2013). For example, significant differences were found even among limpets of the same genus

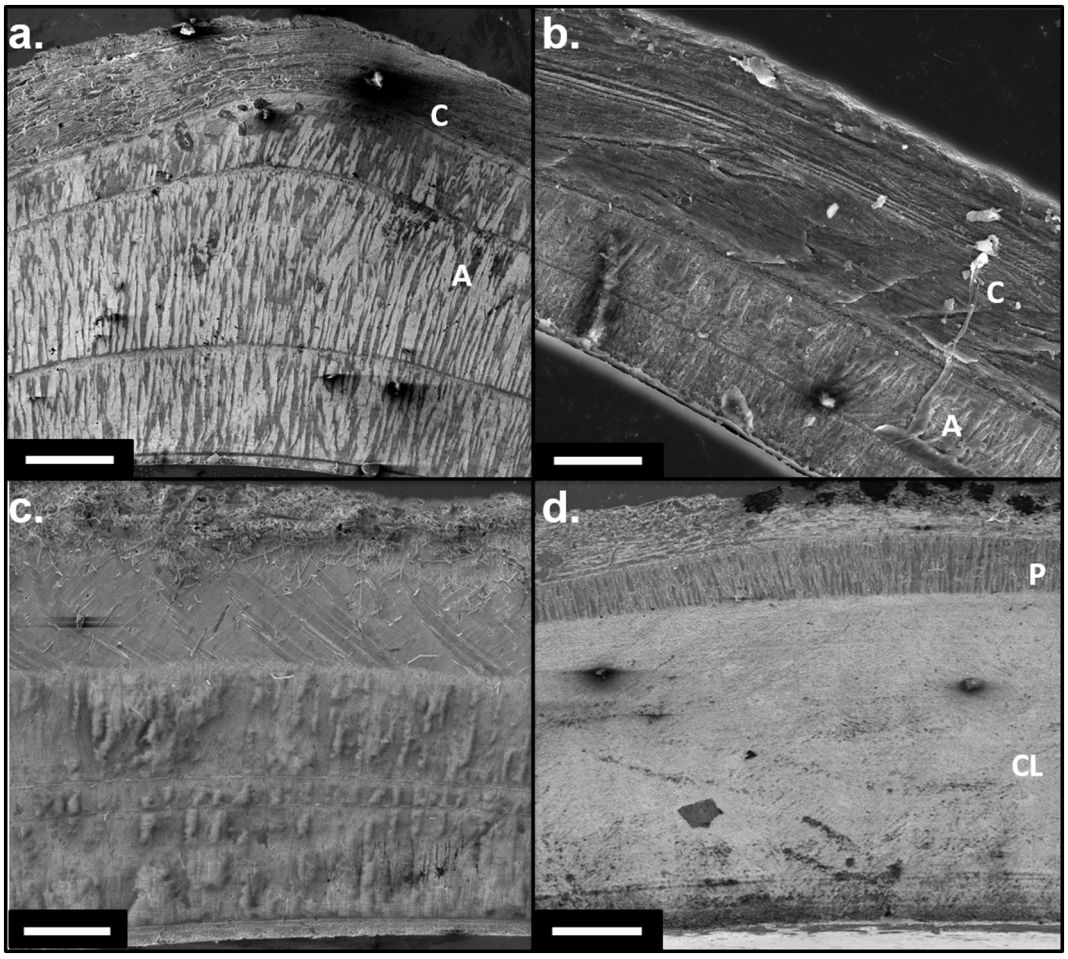

Fig. 5. Scanning electron microscopy of shells from four gastropod species collected at three CO_2 seep sites off Vulcano Island, Italy. (a) *Patella caerulea,* (b) *Patella rustica,* (c) *Hexaplex trunculus,* and (d) *Osilinus turbinatus.* For the two limpets (a,b) aragonite layers are marked with an "A", and calcite layers are marked with a "C." For the whelk (c) and top shell (d) the shells are composed entirely of aragonite. Example of prismatic layer marked with a "P"; crossed-lamellar layer marked with a "CL." Scale bars represent 100 μm.

in the present study. While various properties of the $CaCO_3$ shells appear to be resilient to chronic pH levels as low as 7.7, evidence of dissolution, disorganized and simplified crystallographic arrangement of minerals, and impaired shell integrity suggest challenges to survival in a near future pH environment. We found that the calcite/aragonite ratio varied and increased significantly with chronic exposure to reduced pH in shells of the limpet *P. rustica*. Moreover, each of the four species of gastropods displayed reductions in elasticity or inner shell toughness when collected from the Low pH site. Whether these compromised shell features hinder populations remains to be determined. However, it is noteworthy that Hall-Spencer et al. (2008) found that both the whelk and top-shell snail in the present study were reduced or absent at a separate seep site (Ischia, Italy) at pH levels similar to our Low site. The results presented here depict a situation in which gastropods experience alterations in biomineralization and mechanical properties of their shells. These alterations have the potential to render individuals more susceptible to infection or predation.

Wide varieties of mollusks are highly susceptible to the effects of ocean acidification, including those of high commercial importance (Cooley et al., 2012, 2015). Studies carried out at Mediterranean CO_2 seeps have shown that gastropod species diversity declines as seawater pH levels fall and that pH-tolerant species are often smaller than conspecifics living under ambient pH conditions due to increased physiological stress and shell dissolution (Cigliano et al., 2010; Milazzo et al., 2014; Garilli et al., 2015; Harvey et al., 2016). Laboratory studies on a variety of mollusks have also shown a decrease in calcification, growth, overall body size, abundance and survival in individuals exposed to acidified conditions (reviewed by Kroeker et al., 2013a). The two species of limpets examined in the present study, *P. caerulea* and *P. rustica*, are clearly exceptions to this general trend, as shell length did not decrease with increasing proximity to the CO_2 seeps. Rodolfo-Metalpa et al. (2011) found that *P. caerulea* living at high CO_2 levels were able to upregulate calcification rates to counteract dissolution, and that this adaptation to hypercapnia was retained even when individuals were transplanted to ambient pH conditions. Here, we found that *P. caerulea* demonstrated a statistically non-significant trend towards increased size with decreasing pH, while *P. rustica* significantly increased in shell size with decreasing pH. Ransome (2007) found that although the abundances of *P. caerulea* decreased with declining pH at a CO_2 seep off the island of Ischia, Italy, mean shell length increased significantly. The larger size of *P. caerulea* at low-pH sites at multiple CO_2 seep systems suggests that this species may be reaping the benefits of increased productivity of the microphytobenthos (Johnson et al., 2015). It has been previously demonstrated in mollusks that increased food availability offset decreases in calcification rates and growth due to ocean acidification (Melzner et al., 2011; Thomsen et al., 2013).

A number of investigators have noted that marine invertebrates able to persist in acidified conditions are likely to benefit from decreased competition for the abundant algal food resources known to characterize sites close to seeps (Porzio et al., 2011; Baggini et al., 2015). The larger sizes of *P. caerulea* collected from the site nearest the CO_2 seep may also be the result of individuals allocating greater amounts of

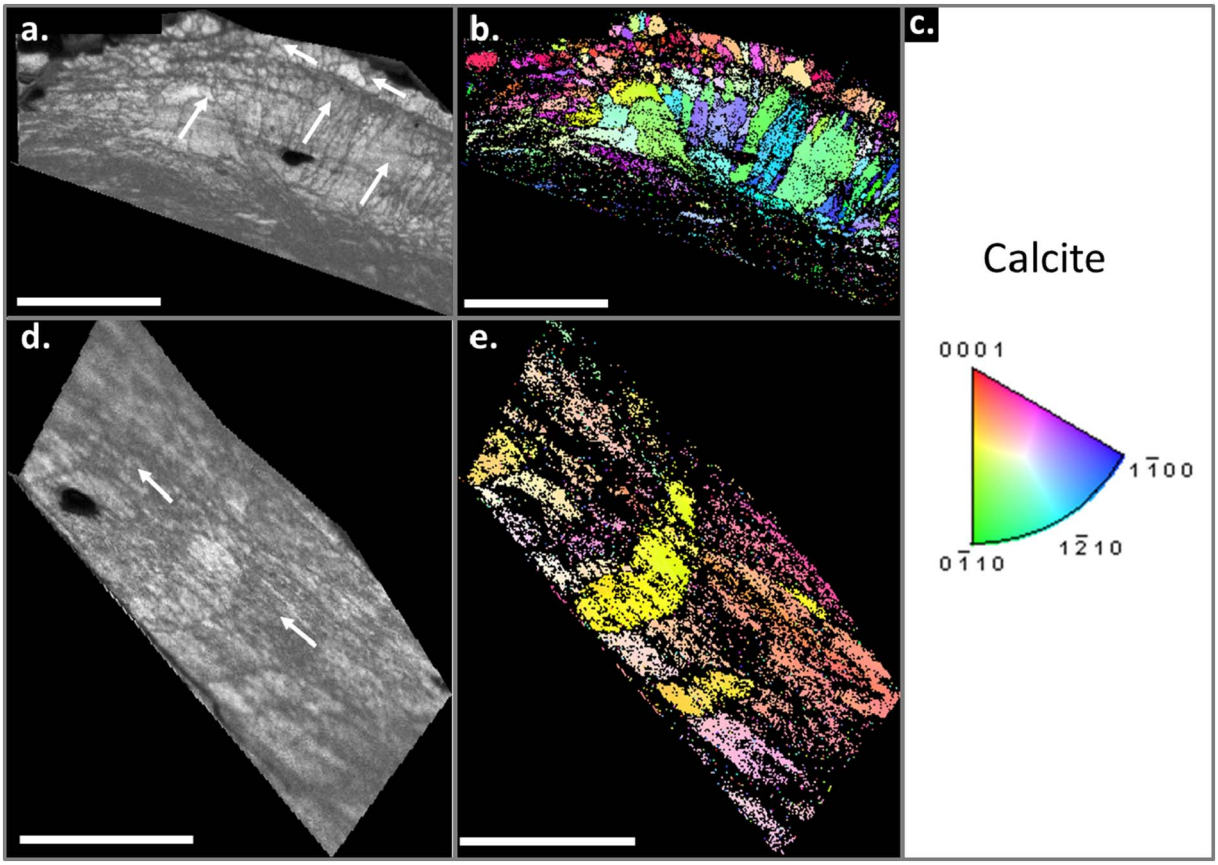

Fig. 6. Electron backscatter diffraction data for sections across the thickness of shells of *Patella caerulea* collected from ambient (a–c) and low (d–e) pH seep sites. (a, d) Diffraction intensity maps of shell section. (b, e) Corresponding crystallographic maps demonstrating the orientation of calcite crystals. (c) Color-key for calcite crystallographic planes. White arrows indicate the preferred orientation of crystals (a, b) Scale bars represent 100 μm. (d–e) Scale bars represent 70 μm.

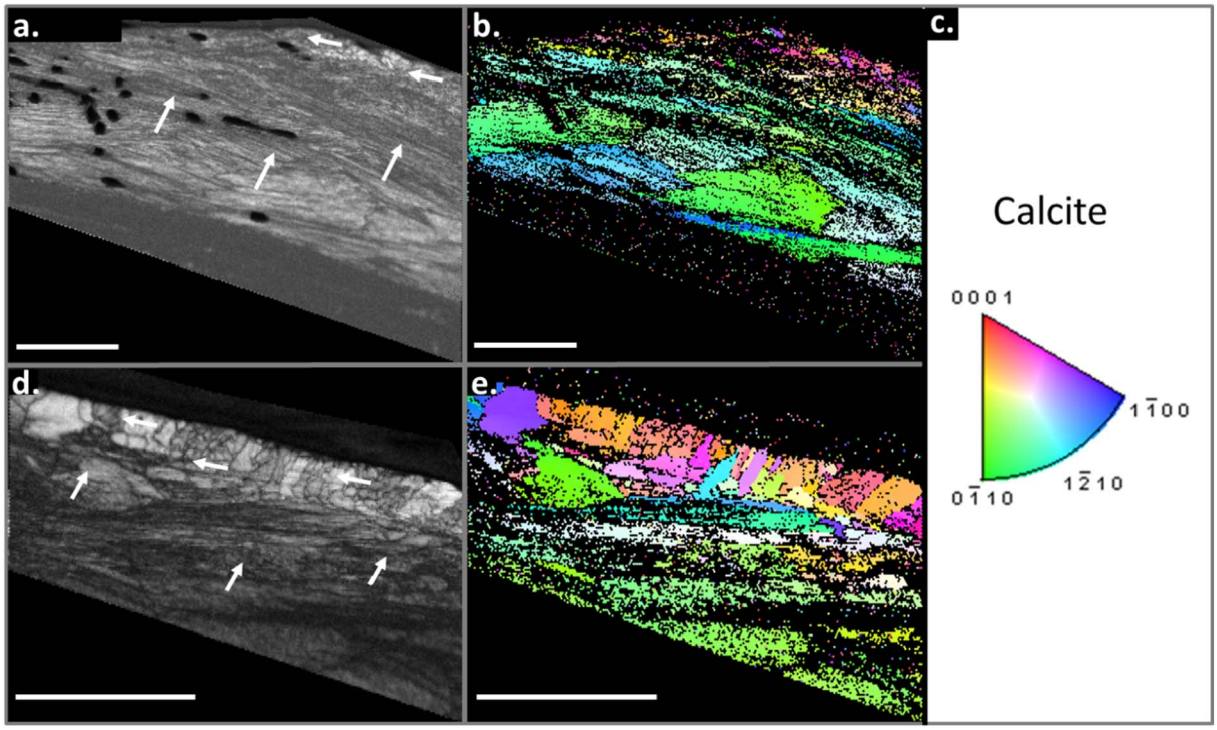

Fig. 7. Electron backscatter diffraction data for sections across the thickness of shells of *Patella rustica* collected from ambient (a–c) and low (d–e) pH sites. (a, d) Diffraction intensity maps of shell sections. (b, e) Corresponding crystallographic maps demonstrating the orientation of calcite crystals. (c) Color-key for calcite crystallographic planes. White arrows indicate the preferred orientation of crystals (a, b). Scale bars represent 100 μm. (d–e) Scale bars represent 90 μm.

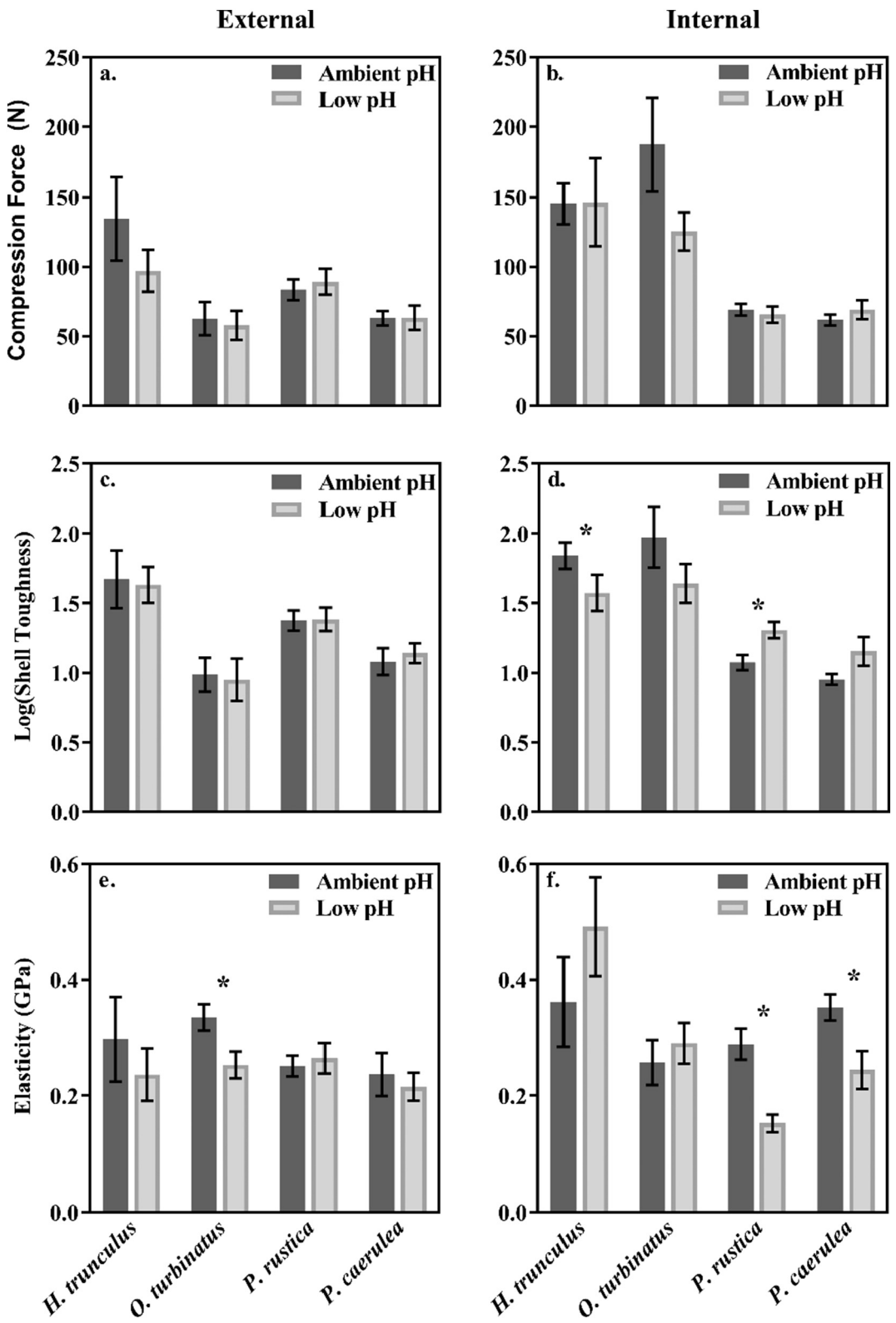

Fig. 8. Material strength characteristics for external (a, c, & e) and internal (b, d, & f) shell surfaces of four gastropod species collected from ambient, moderate, and low pH seep sites. Force (N) required to fracture the shell surface (a & b), log transform of shell surface toughness (J/m) (c–d), elasticity (GPa) of the shell surface (e–f). Bars represent means ± 1SE, for each species at the given pH. Significantly different means ($p < 0.05$) are indicated with an asterisk (*).

energy to shell growth. As shells of juvenile or early adult mollusks are at greater risk of dissolution (Bamber, 1990; Green et al., 2004), limpets may necessarily be compensating by depositing additional shell material that ultimately generates larger shell size in a more acidic environment.

In contrast to the limpets, the top-shell *O. turbinatus* exhibited a significant decrease in shell length with decreasing pH. Similarly, the whelk *Hexaplex trunculus* displayed a trend towards smaller shell size with increasing hypercapnia, which has since been verified statistically by Harvey et al. (2016). Both gastropods have shells composed entirely

of aragonite, a mineral known to be about 1.5 times more soluble than calcite (Mucci, 1983), while containing crystals that are smaller and more densely packed than calcite (Weiner and Addadi, 1997). This difference in crystalline microstructure makes it more energetically demanding to build or replace shell material that is composed of aragonite (Allemand et al., 2011). Combined, these factors increase the challenges for calcified marine invertebrates with aragonite shells to grow to adult size and maintain their shells under low pH stress. Accordingly, the aragonitic shell of new recruits of the reef-building vermetid gastropod *Dendropoma petraeum* transplanted along the CO_2 gradient off Vulcano Island, dissolved at low pH levels (Milazzo et al., 2014). Moreover, the Mg/Ca content of their shells significantly increased in seawater with lowered carbonate ion concentrations, reflecting an impaired ability of the vermetids to remove Mg from haemolymph and extrapallial fluids.

Because there exist differences in the solubility of shells under reduced pH based on their ratio of calcite to aragonite (Milliman, 1974), it is important to evaluate the lability of the ratio of these $CaCO_3$ polymorphs at the three pH sites sampled in the present study. The two limpets in the present study, *P. caerulea* and *P. rustica,* demonstrated varying responses in mineralogy to chronic exposure to ocean acidification. *Patella rustica* exhibited a significant increase in shell calcite content at the low pH site, while *P. caerulea* exhibited no change in mineralogy across all three sites. These observations were contrary to our expectations, as two previous studies of *P. caerulea* found that individuals counteract dissolution of their shells in reduced pH seawater by up-regulating calcification, resulting in a thickening of the shell's aragonite layer (Rodolfo-Metalpa et al., 2011; Langer et al., 2014). It is possible that *P. rustica* exposed to ocean acidification has the flexibility to alter its mineralogy such that levels of calcite, a more stable and less soluble polymorph of $CaCO_3$, are increased relative to aragonite. Similarly, Ries (2011) found that the serpulid polychaete *Hydroides crucigera* and the whelk *Urosalpinx cinerea* increased the proportions of calcite to aragonite in their shells in response to increased pCO_2. Ries (2011) postulates that difficulty in maintaining a supersaturated condition at the site of calcification due to acidosis could be responsible for the preferential production of calcite over aragonite. Because aragonite is more soluble than calcite, the site of calcification becomes undersaturated with respect to aragonite earlier than calcite.

Patella caerulea may be responding in the same way as *P. rustica*, but higher levels of dissolution of the external calcite due to the lack of a periostracum actually outweigh the production of calcite. Beniash et al. (2010) found that the oyster *Crassostrea virginica* demonstrated decreased shell mass with no corresponding decrease in shell size. The authors suggest that while the organism is still able to biomineralize, either dissolution of the external shell or increased energetic demand led to thinner shells being constructed. While no data was collected for shell thickness, the same disruption in the balance between dissolution and production could contribute to the mineralogy ratio in *P. caerulea.* Future studies of these limpet species should include an investigation into the shell thickness across the three sampling sites. As demonstrated by Langer et al. (2014), this would help determine which layer (calcite or aragonite) demonstrates changes in response to ocean acidification and exactly what those changes encompass.

The morphology, arrangement, and orientation of the calcite or aragonite crystals can also affect shell solubility under acidified conditions (Harper, 2000). While the morphology of individual crystals was not investigated in the present study, we did identify several shell microstructures (prismatic, crossed lamellar) as well as alterations in calcite crystal orientation in limpet shells. However, it is important to note that these analyses were carried out with a single representative shell from each different pH site and need to be further verified with larger sample sizes. Although electron backscatter diffraction analysis of aragonitic shell microstructures is possible, including those of limpets (e.g., Suzuki et al., 2010), the absence of sufficient diffraction and continuous data prevented the use of this technique to examine the aragonitic shells of the top-shell snail and whelk and the aragonite layers of the limpet shells. While electron backscatter diffraction data presented in the present study must be cautiously interpreted given small sample size, the observed change in crystal orientation in the shell of *P. caerulea* (lacking a protective periostracum) collected at the low pH site could be indicative of a crystallographic response to ocean acidification. Several studies have shown that shell ultrastructure can be altered, and the level of disorganization of calcite or aragonite crystals increased, under conditions of ocean acidification (Welladsen et al., 2010; Hahn et al., 2012; Fitzer et al., 2014; Li et al., 2014).

Finally, three measures of the material properties of shells in all four gastropod species were employed to determine quantitatively if shell integrity is compromised with chronic exposure to reduced pH. Despite visible evidence of dissolution of external surfaces of shells collected for all species from the Low site, no significant reduction in the force required to fracture shells was observed. Taken alone, this could be indicative of a resilience of mechanical strength to ocean acidification. However, given the impacts observed in the present study on the reduced integrity (elasticity and toughness) of the internal shell surfaces, this is unlikely. Welladsen et al. (2010) reported that while exposure to near-future levels of ocean acidification decreased the force required to crush the shell of the oyster *Pinctada fucata*, there was no change in the force needed to initially fracture (crack) the shell. While no significant change in the force necessary to fracture shells was seen between gastropods collected from our Low and Ambient sites, it is possible that additional measures of shell strength such as crushing compression may have revealed a decrease in force required to crush shells of individuals living at the Low pH site.

Changes to internal shell surface integrity suggests either dissolution is occurring or calcification is impaired due to physiological stress associated with a low pH environment or the undersaturation of aragonite that characterizes the Low site (Milazzo et al., 2014). For example, Welladsen et al. (2010) reported that the aragonitic inner shell layer of the pearl oyster *Pinctada fucata* became disorganized, with crystal structures developing as misshapen and irregular when chronically exposed to reduced pH. The resulting aragonite layer had decreased shell integrity. While crystal structure was not investigated for the aragonite layers in this study, it is possible that the altered shell integrity observed is a response to impaired biomineralization of the inner aragonite shell layer. Aragonite requires a greater energetic investment to produce than calcite (Allemand et al., 2011), so pH stress may reduce the capacity to maintain or produce the inner shell surface. Costs of shell maintenance and production are not trivial. For example, the cost of producing the organic matrix within calcium carbonate can cost an organism 10–60% of the energy invested in somatic growth, and the polymorph aragonite has a higher level of organic material within its matrix than does calcite (Palmer, 1992). Aragonite that is less tough or less elastic because of insufficient energy for biomineralization could render the gastropods more susceptible to predation. Both crabs and sea birds have been observed to pry or chip at the edges of limpet shells to gain access to the soft body tissues (Coleman et al., 1999). Reduced shell elasticity may compromise the ability to withstand such predator attacks, as well as those from crushing predators. *H. trunculus* is unique among the four gastropods examined as it not only depends on its shell as refuge from predators, but uses the toothed lip of the shell aperture to chip off the shells margins of prospective prey including gastropods and bivalves (Peharda and Morton, 2006; Morton et al., 2007). With high levels of dissolution and pitting observed in the external shell and the decreased toughness of the internal shell detected, it is likely that a shell-chipping mode of predation will be compromised. Should *H. trunculus*, whose shell integrity at the Low pH site was compromised by gaping holes exposing soft tissues, suffer population level mortality from future infectious disease, trophic dynamics are likely to shift significantly as a top predatory carnivore on gastropods and bivalves is removed from the community.

Acknowledgements

We thank Gopi Samudrala and Yogesh Vohra for their assistance with X-ray diffraction measurements performed in the UAB Department of Physics, as well as William Monroe in the UAB SEM Facility of the Department of Materials Science and Engineering. We also extend our gratitude to Margaret Amsler for assistance with sample and manuscript preparations. We thank Raya Berman and Michelle Gannon in the Department of Geology at the University of Alabama for their aid with electron backscatter diffraction analyses. Finally, we thank Justin Ries and Isaac Westfield for assistance with material strength analyses carried out in the Department of Marine and Environmental Sciences at Northeastern University. The present study was supported in part by National Science Foundation grant ANT-1041022 awarded to JBM, CDA, and Robert A. Angus. JBM acknowledges support provided by the UAB Endowed Professorship in Polar and Marine Biology.

References

Allemand, D., Tambutté, É., Zoccola, D., Tambutté, S., 2011. Coral calcification, cells to reefs. In: Coral Reefs: An Ecosystem in Transition. Springer, pp. 119–150.

Baggini, C., Issaris, Y., Salomidi, M., Hall-Spencer, J., 2015. Herbivore diversity improves benthic community resilience to ocean acidification. J. Exp. Mar. Biol. Ecol. 469, 98–104. http://dx.doi.org/10.1016/j.jembe.2015.04.019.

Bamber, R., 1990. The effects of acidic seawater on three species of lamellibranch mollusc. J. Exp. Mar. Biol. Ecol. 143, 181–191. http://dx.doi.org/10.1016/0022-0981(90)90069-O.

Beniash, E., Ivanina, A., Lieb, N.S., Kurochkin, I., Sokolova, I.M., 2010. Elevated level of carbon dioxide affects metabolism and shell formation in oysters *Crassostrea virginica*. Mar. Ecol. Prog. Ser. 419, 95–108. http://dx.doi.org/10.3354/meps08841.

Boatta, F., D'Alessandro, W., Gagliano, A., Liotta, M., Milazzo, M., Rodolfo-Metalpa, R., Hall-Spencer, J., Parello, F., 2013. Geochemical survey of Levante Bay, Vulcano Island (Italy), a natural laboratory for the study of ocean acidification. Mar. Pollut. Bull. 73, 485–494. http://dx.doi.org/10.1016/j.marpolbul.2013.01.029.

Boucetta, S., Derbal, F., Boutiba, Z., Kara, M.H., 2010. First biological data on the marine snails *Oscilinus turbinatus* (Gastropoda, Trochidae) of eastern coasts of Algeria. In: Ceccaldi, H.J., Dekeyser, I., Girault, M., Stora, G. (Eds.), Global Change: Mankind-Marine Environment Interactions. Springer, Dordrecht.

Bray, L., Pancucci-Papadopulou, M.A., Hall-Spencer, J.M., 2014. Sea urchin response to rising pCO_2 shows ocean acidification may fundamentally alter the chemistry of marine skeletons. Med. Mari. Sci. 15 (3), 510–519. http://dx.doi.org/10.12681/mms.579.

Cigliano, M., Gambi, M., Rodolfo-Metalpa, R., Patti, F., Hall-Spencer, J., 2010. Effects of ocean acidification on invertebrate settlement at volcanic CO_2 vents. Mar. Biol. 157, 2489–2502. http://dx.doi.org/10.1007/s00227-010-1513-6.

Coleman, R.A., Goss-Custard, J.D., dit Durell, S.E.L.V., Hawkins, S.J., 1999. Limpet *Patella* spp. consumption by oystercatchers *Haematopus ostralegus*: a preference for solitary prey items. Mar. Ecol. Prog. Ser. 183, 253–261.

Coleman, D.W., Byrne, M., Davis, A.R., 2014. Molluscs on acid: gastropod shell repair and strength in acidifying oceans. Mar. Ecol. Prog. Ser. 509, 203–211. http://dx.doi.org/10.3354/meps10887.

Collard, M., Rastrick, S.P., Calosi, P., Demolder, Y., Dille, J., Findlay, H.S., Hall-Spencer, J.M., Milazzo, M., Moulin, L., Widdicombe, S., 2016. The impact of ocean acidification and warming on the skeletal mechanical properties of the sea urchin *Paracentrotus lividus* from laboratory and field observations. ICES J. Mar. Sci. 73 (3), 727–738. http://dx.doi.org/10.1093/icesjms/fsv018.

Cooley, S.R., Lucey, N., Kite-Powell, H., Doney, S.C., 2012. Nutrition and income from molluscs today imply vulnerability to ocean acidification tomorrow. Fish Fish. 13, 182–215. http://dx.doi.org/10.1111/j.1467-2979.2011.00424.x.

Cooley, S.R., Rheuban, J.E., Hart, D.R., Luu, V., Glover, D.M., Hare, J.A., Doney, S.C., 2015. An integrated assessment model for helping the United States sea scallop (*Placopecten magellanicus*) fishery plan ahead for ocean acidification and warming. PLoS One 10, e0124145. http://dx.doi.org/10.1371/journal.pone.0124145.

Della Santina, P., Sonni, C., Sartoni, G., Chelazzi, G., 1993. Food availability and diet composition of three coexisting Mediterranean limpets (*Patella* spp.). Mar. Biol. 116, 87–95.

Dubois, P., 2014. The skeleton of postmetamorphic echinoderms in a changing world. Biol. Bull. 226 (3), 223–236.

Fabricius, K., De'ath, G., Noonan, S., Uthicke, S., 2014. Ecological effects of ocean acidification and habitat complexity on reef-associated macroinvertebrate communities. Proc. R. Soc. Lond. B 281, 20132479. http://dx.doi.org/10.1098/rspb.2013.2479.

Fitzer, S.C., Phoenix, V.R., Cusack, M., Kamenos, N.A., 2014. Ocean acidification impacts mussel control on biomineralisation. Sci Rep 4. http://dx.doi.org/10.1038/srep06218.

Garilli, V., Rodolfo-Metalpa, R., Scuderi, D., Brusca, L., Parrinello, D., Rastrick, S.P., Foggo, A., Twitchett, R.J., Hall-Spencer, J.M., Milazzo, M., 2015. Physiological advantages of dwarfing in surviving extinctions in high-CO_2 oceans. Nat. Clim. Chang. 5, 678–682. http://dx.doi.org/10.1038/nclimate2616.

Gaylord, B., Kroeker, K.J., Sunday, J.M., Anderson, K.M., Barry, J.P., Brown, N.E., Connell, S.D., Dupont, S., Fabricius, K.E., Hall-Spencer, J.M., 2015. Ocean acidification through the lens of ecological theory. Ecology 96, 3–15. http://dx.doi.org/10.1890/14-0802.1.

Gazeau, F., Quiblier, C., Jansen, J.M., Gattuso, J.-P., Middelburg, J.J., Heip, C.H.R., 2007. Impact of elevated CO_2 on shellfish calcification. Geophys. Res. Lett. 34 (7), L07603. http://dx.doi.org/10.1029/2006GL028554.

Green, M.A., Jones, M.E., Boudreau, C.L., Moore, R.L., Westman, B.A., 2004. Dissolution mortality of juvenile bivalves in coastal marine deposits. Limnol. Oceanogr. 49, 727–734.

Hahn, S., Rodolfo-Metalpa, R., Griesshaber, E., Schmahl, W.W., Buhl, D., Hall-Spencer, J., Baggini, C., Fehr, K., Immenhauser, A., 2012. Marine bivalve shell geochemistry and ultrastructure from modern low pH environments: environmental effect versus experimental bias. Biogeosciences 9, 1897–1914. http://dx.doi.org/10.5194/bg-9-1897-2012.

Hall-Spencer, J.M., Rodolfo-Metalpa, R., Martin, S., Ransome, E., Fine, M., Turner, S.M., Rowley, S.J., Tedesco, D., Buia, M.-C., 2008. Volcanic carbon dioxide vents show ecosystem effects of ocean acidification. Nature 454, 96–99. http://dx.doi.org/10.1038/nature07051.

Harper, E.M., 2000. Are calcitic layers an effective adaptation against shell dissolution in the Bivalvia? J. Zool. 251 (2), 179–186. http://dx.doi.org/10.1111/j.1469-7998.2000.tb00602.x.

Harvey, B.P., McKeown, N.J., Rastrick, S.P., Bertolini, C., Foggo, A., Graham, H., Hall-Spencer, J.M., Milazzo, M., Shaw, P.W., Small, D.P., 2016. Individual and population-level responses to ocean acidification. Sci Rep 6. http://dx.doi.org/10.1038/srep20194.

Hoegh-Guldberg, O., Cai, R., Poloczanska, E.S., Brewer, P.G., Sundby, S., Hilmi, K., Fabry, V.J., Jung, S., 2014. The ocean. In: Barros, V.R., Field, C.B., Dokken, D.J., Mastrandrea, M.D., Mach, K.J., Bilir, T.E., Chatterjee, M., Ebi, K.L., Estrada, Y.O., Genova, R.C., Girma, B., Kissel, E.S., Levy, A.N., S, MacCracken, Mastrandrea, P.R., White, L.L. (Eds.), Climate Change 2014: Impacts, Adaptation, and Vulnerability. Part B: Regional Aspects. Contribution of Working Group II to the Fifth Assessment Report of the Intergovernmental Panel on Climate Change. Cambridge University Press, Cambridge, United Kingdom and New York, NY, USA, pp. 1655–1731.

Inoue, S., Kayanne, H., Yamamoto, S., Kurihara, H., 2013. Spatial community shift from hard to soft corals in acidified water. Nat. Clim. Chang. 3, 683–687. http://dx.doi.org/10.1038/nclimate1855.

IPCC, 2013. Summary for policymakers. In: Stocker, T.F., Qin, D., Plattner, G.-K., Tignor, M., Allen, S.K., Boschung, J., Nauels, A., Xia, Y., Bex, V., Midgley, P.M. (Eds.), Climate Change 2013: The Physical Science Basis. Contribution of Working Group I to the Fifth Assessment Report of the Intergovernmental Panel on Climate Change. Cambridge University Press, Cambridge, United Kingdom and New York, NY, USA. http://dx.doi.org/10.1017/CBO9781107415324.004.

Johnson, V.R., Brownlee, C., Milazzo, M., Hall-Spencer, J.M., 2015. Marine microphytobenthic assemblage shift along a natural shallow-water CO_2 gradient subjected to multiple environmental stressors. J.Mar. Sci. Eng. 3, 1425–1447. http://dx.doi.org/10.3390/jmse3041425.

Kroeker, K.J., Kordas, R.L., Crim, R., Hendriks, I.E., Ramajo, L., Singh, G.S., Duarte, C.M., Gattuso, J.P., 2013a. Impacts of ocean acidification on marine organisms: quantifying sensitivities and interaction with warming. Glob. Chang. Biol. 19, 1884–1896. http://dx.doi.org/10.1111/gcb.12179.

Kroeker, K.J., Micheli, F., Gambi, M.C., 2013b. Ocean acidification causes ecosystem shifts via altered competitive interactions. Nat. Clim. Chang. 3, 156–159. http://dx.doi.org/10.1038/nclimate1680.

Langer, G., Nehrke, G., Baggini, C., Rodolfo-Metalpa, R., Hall-Spencer, J., Bijma, J., 2014. Limpets counteract ocean acidification induced shell corrosion by thickening of aragonitic shell layers. Biogeosciences 11, 7363–7368. http://dx.doi.org/10.5194/bg-11-7363-2014.

Lardies, M.A., Aria, M.B., Poupin, J.H., Manriquez, P.H., Torres, R., Vargas, C.A., Navarro, J.M., Lagos, N.A., 2014. Differential response to ocean acidification in physiological traits of *Concholepas concholepas* populations. J. Sea Res. 90, 127–134.

Lécuyer, C., Hutzler, A., Amiot, R., Daux, V., Grosheny, D., Otero, O., Martineau, F., Fourel, F., Balter, V., Reynard, B., 2012. Carbon and oxygen isotope fractionations between aragonite and calcite of shells from modern molluscs. Chem. Geol. 332–333, 92–101. http://dx.doi.org/10.1016/j.chemgeo.2012.08.034.

Li, C., Chan, V., He, C., Meng, Y., Yao, H., Shih, K., Thiyagarajan, V., 2014. Weakening mechanisms of the serpulid tube in a high-CO_2 world. Environ. Sci. Technol. 48, 14158–14167. http://dx.doi.org/10.1021/es501638h.

Mannino, M.A., Thomas, K.D., Leng, M.J., Sloane, H.J., 2008. Shell growth and oxygen isotopes in the topshell *Osilinus turbinatus*: resolving past inshore sea surface temperatures. Geo-Mar Lett 309–326. http://dx.doi.org/10.1007/s00367-008-0107-5.

McClintock, J.B., Amsler, M.O., Angus, R.A., Challener, R.C., Schram, J.B., Amsler, C.D., Mah, C.L., Cuce, J., Baker, B.J., 2011. The Mg-calcite composition of Antarctic echinoderms: important implications for predicting the impacts of ocean acidification. J. Geol. 119, 457–466. http://dx.doi.org/10.1086/660890.

Melatunan, S., Calosi, P., Rundle, S.D., Widdicombe, S., Moody, A.J., 2013. Effects of ocean acidification and elevated temperature on shell plasticity and its energetic basis in an intertidal gastropod. Mar. Ecol. Prog. Ser. 472, 155–168. http://dx.doi.org/10.3354/meps10046.

Melzner, F., Stange, P., Trübenbach, K., Thomsen, J., Casties, I., Panknin, U., Gorb, S., Gutowska, M.A., 2011. Food supply and seawater pCO_2 impact calcification and internal shell dissolution in the blue mussel *Mytilus edulis*. PLoS One 6, e24223. http://dx.doi.org/10.1371/journal.pone.0024223.

Milazzo, M., Rodolfo-Metalpa, R., San Chan, V.B., Fine, M., Alessi, C., Thiyagarajan, V., Hall-Spencer, J.M., Chemello, R., 2014. Ocean acidification impairs vermetid reef recruitment. Sci Rep 4. http://dx.doi.org/10.1038/srep04189.

Milliman, J., 1974. Marine Carbonates, Part I. Springer-Verlag, New York.

Morton, B., Peharda, M., Harper, E., 2007. Drilling and chipping patterns of bivalve prey

predation by *Hexaplex trunculus* (Mollusca: Gastropoda: Muricidae). J. Mar. Biol. Assoc. UK 87, 933–940. http://dx.doi.org/10.1017/S0025315407056184.

Mucci, A., 1983. The solubility of calcite and aragonite in seawater at various salinities, temperatures, and one atmosphere total pressure. Am. J. Sci. 283, 780–799. http://dx.doi.org/10.2475/ajs.283.7.780.

Nakicenovic, N., Swart, R., 2000. Special report on emissions scenarios. In: Nakicenovic, Nebojsa, Swart, Robert (Eds.), Special Report on Emissions Scenarios. Cambridge University Press, Cambridge, UK, 0521804930, pp. 612 (July 2000 1).

Newcomb, L.A., Milazzo, M., Hall-Spencer, J.M., Carrington, E., 2015. Ocean acidification bends the mermaid's wineglass. Biol. Lett. 11, 20141075. http://dx.doi.org/10.1098/rsbl.2014.1075.

Palmer, A.R., 1992. Calcification in marine molluscs: how costly is it? Proc. Natl. Acad. Sci. 89, 1379–1382.

Parker, L.M., Ross, P.M., O'Connor, W.A., Pörtner, H.O., Scanes, E., Wright, J.M., 2013. Predicting the response of molluscs to the impact of ocean acidification. Biology 2, 651–692. http://dx.doi.org/10.3390/biology2020651.

Peharda, M., Morton, B., 2006. Experimental prey species preferences of *Hexaplex trunculus* (Gastropoda: Muricidae) and predator–prey interactions with the black mussel *Mytilus galloprovincialis* (Bivalvia: Mytilidae). Mar. Biol. 148, 1011–1019. http://dx.doi.org/10.1007/s00227-005-0148-5.

Pérez-Huerta, A., Cusack, M., 2009. Optimizing electron backscatter diffraction of carbonate biominerals—resin type and carbon coating. Microsc. Microanal. 15, 197–203. http://dx.doi.org/10.1017/S1431927609090370.

Pérez-Huerta, A., Dauphin, Y., Cuif, J.P., Cusack, M., 2011. High resolution electron backscatter diffraction (EBSD) data from calcite biominerals in recent gastropod shells. Micron 42, 246–251. http://dx.doi.org/10.1016/j.micron.2010.11.003.

Porzio, L., Buia, M.C., Hall-Spencer, J.M., 2011. Effects of ocean acidification on macroalgal communities. J. Exp. Mar. Biol. Ecol. 400, 278–287. http://dx.doi.org/10.1016/j.jembe.2011.02.011.

R Development Core Team, 2016. R: A Language and Environment for Statistical Computing. R Foundation for Statistical Computing, Vienna, Austria.

Ransome, E., 2007. Determining the Effects of Ocean Acidification on Intertidal Organisms. MS Thesis. University of Plymouth, Plymouth, UK.

Ries, J.B., 2011. Skeletal mineralogy in a high-CO_2 world. J. Exp. Mar. Biol. Ecol. 403, 54–64. http://dx.doi.org/10.1016/j.jembe.2011.04.006.

Ries, J.B., Cohen, A.L., McCorkle, D.C., 2009. Marine calcifiers exhibit mixed responses to CO_2-induced ocean acidification. Geology 37, 1131–1134. http://dx.doi.org/10.1130/G30210A.1.

Roberts, D.A., Birchenough, S.N.R., Lewis, C., Sanders, M.B., Bolam, T., Sheahan, D., 2013. Ocean acidification increases the toxicity of contaminated sediments. Glob. Chang. Biol. 19, 340–351. http://dx.doi.org/10.1111/gcb.12048.

Rodolfo-Metalpa, R., Houlbrèque, F., Tambutté, É., Boisson, F., Baggini, C., Patti, F.P., Jeffree, R., Fine, M., Foggo, A., Gattuso, J., 2011. Coral and mollusc resistance to ocean acidification adversely affected by warming. Nat. Clim. Chang. 1, 308–312. http://dx.doi.org/10.1038/nclimate1200.

Rodolfo-Metalpa, R., Montagna, P., Aliani, S., Borghini, M., Canese, S., Hall-Spencer, J.M., Foggo, A., Milazzo, M., Taviani, M., Houlbrèque, F., 2015. Calcification is not the Achilles' heel of cold-water corals in an acidifying ocean. Glob. Chang. Biol. 21, 2238–2248. http://dx.doi.org/10.1111/gcb.12867.

Shirayama, Y., Thornton, H., 2005. Effect of increased atmospheric CO_2 on shallow water marine benthos. J. Geophys. Res. 110 (C09S08). http://dx.doi.org/10.1029/2004JC002618.

Suzuki, M., Kameda, J., Sasaki, T., Saruwatari, K., Nagasawa, H., Kogure, T., 2010. Characterization of the multilayered shell of a limpet, *Lottia kogamogai* (Mollusca: Patellogastropoda), using SEM–EBSD and FIB–TEM techniques. J. Struct. Biol. 171, 223–230. http://dx.doi.org/10.1016/j.jsb.2010.04.008.

Thomsen, J., Casties, I., Pansch, C., Körtzinger, A., Melzner, F., 2013. Food availability outweights ocean acidification effects in juvenile *Mytilus edulis*: laboratory and field experiments. Glob. Chang. Biol. 19, 1017–1027. http://dx.doi.org/10.1111/gcb.12109.

Vizzini, S., Leonado, R.D., Costa, V., Tramati, C.D., Luzzu, F., Mazzola, A., 2013. Trace element bias in the use of CO_2 vents as analogues for low pH environments: implications for contamination levels in acidified oceans. Estuar. Coast. Shelf Sci. 134, 19–30. http://dx.doi.org/10.1016/j.ecss.2013.09.015.

Weiner, S., Addadi, L., 1997. Design strategies in mineralized biological materials. J. Mater. Chem. 7, 689–702. http://dx.doi.org/10.1039/A604512J.

Welladsen, H.M., Southgate, P.C., Heimann, K., 2010. The effects of exposure to near-future levels of ocean acidification on shell characteristics of *Pinctada fucata* (Bivalvia: Pteriidae). Molluscan Res. 30, 125.